Xiong, C., Huang, Y., Wang, F., Lühr, H., Zhou, Y., Zhu, J. (2025): Responses of the Ionospheric Zonal Currents From Equator to Middle Latitudes During the Intense Geomagnetic Storm on 10–12 May 2024. - Journal of Geophysical Research: Space Physics, 130, 7, e2025JA033992.

https://doi.org/10.1029/2025JA033992

JGR Space Physics

RESEARCH ARTICLE
10.1029/2025JA033992

Special Collection:
Space Weather Events of 2024 May 9-15

Responses of the Ionospheric Zonal Currents From Equator to Middle Latitudes During the Intense Geomagnetic Storm on 10–12 May 2024

Chao Xiong[1], Yuyang Huang[1], Fengjue Wang[1], Hermann Lühr[2], Yunliang Zhou[1], and Jia Zhu[1]

[1]School of Earth and Space Science and Technology, Wuhan University, Wuhan, China, [2]Section 2.3, GFZ Helmholtz Centre for Geosciences, Potsdam, Germany

Key Points:

- Extreme intense EEJ values, reaching 300 and −400 mA/m, have been observed during the storm main and recovery phases
- The zonal currents at low and middle latitudes showed prominent dependence on LT
- Two eastward zonal current jets were found located at ±25° MLat, emerged with westward zonal currents at low and middle latitudes at the dusk sector

Correspondence to:
Y. Zhou,
zhouyl@whu.edu.cn

Citation:
Xiong, C., Huang, Y., Wang, F., Lühr, H., Zhou, Y., & Zhu, J. (2025). Responses of the ionospheric zonal currents from equator to middle latitudes during the intense geomagnetic storm on 10–12 May 2024. *Journal of Geophysical Research: Space Physics*, *130*, e2025JA033992. https://doi.org/10.1029/2025JA033992

Received 23 MAR 2025
Accepted 17 JUN 2025

Author Contributions:
Conceptualization: Chao Xiong, Hermann Lühr
Data curation: Yuyang Huang, Yunliang Zhou
Formal analysis: Chao Xiong
Investigation: Chao Xiong, Fengjue Wang
Methodology: Chao Xiong, Yuyang Huang, Hermann Lühr, Yunliang Zhou
Visualization: Yuyang Huang, Fengjue Wang, Jia Zhu
Writing – original draft: Chao Xiong, Yuyang Huang, Fengjue Wang
Writing – review & editing: Chao Xiong, Yuyang Huang, Fengjue Wang, Hermann Lühr, Yunliang Zhou, Jia Zhu

Abstract In this study, we performed a detailed analysis of the ionospheric zonal currents from equator to middle latitudes during the recent intense geomagnetic storm on 10–12 May 2024. Magnetic measurements from two ground stations in the America sector as well as those from the Swarm satellites have been used. Extreme intensified eastward and westward EEJ values reaching 300 and −400 mA/m have been observed during the storm main and recovery phases, respectively. Such intense EEJ values have never been observed during the past 11-year flying period of Swarm mission. In addition, the storm responses of zonal currents at low and middle latitudes have been analyzed using the vertical magnetic field component from Swarm. These zonal currents showed quite prominent dependence on magnetic local time. In the noon sector, eastward currents were dominated under both quiet and storm conditions, with slight intensification during the storm. Conversely, the zonal currents in the dawn and dusk sectors displayed abrupt current reversals within 30 min after the storm sudden commencement, characterized by sustained eastward (dawn) and westward (dusk) perturbations persisting for the rest of one and a half days. Most interestingly, two eastward zonal current jets were found located at ±25° magnetic latitudes at the dusk sector and emerged with westward zonal currents at other low and middle latitudes. We speculate that a shear layer of zonal eastward winds is needed at a conjugate altitude to cause the narrow eastward current jets. To our knowledge, this is the first report of such narrow current jets at middle latitudes during storms.

1. Introduction

Geomagnetic storms are one of the important reasons that cause the ionosphere to differ significantly from its quiet-day climatological patterns. During storms, the convection electric field, set up by the interaction between the solar wind plasma and the magnetosphere, maps into the ionosphere and produces a dawn-to-dusk electric field at high latitudes (Blanc & Caudal, 1985; Heppner, 1972). Under favorable orientation of the interplanetary magnetic field (IMF), for example, the south turning of the IMF Bz component, the dawn-to-dusk electric field can penetrate to middle and low latitudes, which has been often named prompt penetration electric field (PPEF) (e.g., Kikuchi et al., 1996; Nishida, 1968). In the meanwhile, the expansion of the neutral atmosphere at high latitudes produces equatorward winds, which turn westward at middle and low latitudes owing to the Coriolis force. When reaching the low and equatorial latitudes, the disturbance winds generate additional electric fields, which have been named disturbance dynamo electric fields (DDEF) (e.g., Blanc & Richmond, 1980; Xiong et al., 2015).

Though the PPEF and DDEF have been widely used in explaining the ionospheric responses at low and middle latitudes during geomagnetic storms, the two mechanisms work at different stages of a storm and cause different polarizations of electric fields at different local time (LT) sectors (e.g., Scherliess & Fejer, 1997; Xiong et al., 2016; Yamazaki & Kosch, 2015). As reported by Fejer et al. (2008), the PPEF dominates during the initial and main phases of the storm, while several hours later after the storm sudden commencement (SSC), for example, statistically 3–4 hr later (Xiong et al., 2015), the westward disturbance winds arrive at low and equatorial latitudes and then the DDEF dominates. For the LT dependences, the PPEF has generally the same polarization as that generated through the quiet-time E-region wind dynamo, namely eastward during and daytime and westward during nighttime; while the DDEF in general has the opposite polarizations. As a result, it is reasonable to conclude that the final polarization of electric fields at low and equatorial latitudes during storm periods depends on the balance between quiet-time wind dynamo, PPEF and DDEF.

The equatorial electrojet (EEJ), a strong zonal current found in the ionospheric E-region over the dip equator, is strongly disturbed during geomagnetic storms (Xiong et al., 2016; Yamazaki & Kosch, 2015). Given that the EEJ intensity is directly related to the low-latitude electric field strength, the EEJ serves as an ideal indicator for understanding and characterizing the instantaneous response of low-latitude currents to the disturbed electric fields during geomagnetic storms. Manoj and Maus (2012) developed a real-time forecast service for the ionospheric equatorial zonal electric field, which is crucial for the understanding the dynamic variations of the EEJ. Studies have shown that during the storm initial and main phases, EEJ can be significantly enhanced or even reversed, while during the storm recovery phase, the weakening EEJ or counter electrojet (CEJ) can also be observed (Le Huy & Amory-Mazaudier, 2005; Yamazaki & Kosch, 2015). All these observations reveal that the disturbed electric fields at low latitudes are much more complex than those simply attributed to PPEF and DDEF.

An intense geomagnetic storm happened on 10–12 May 2024, which was the most intense geomagnetic storm happened during the past 20 years. Several studies have investigated the ionospheric responses during this intense storm. For instance, Carmo et al. (2024) observed a persistent, westward-propagating, large-scale equatorial plasma bubble over Latin America, alongside an enhanced nighttime super fountain effect and a positive ionospheric storm. Furthermore, Huang et al. (2024) discovered a peculiar westward-moving nighttime enhancement of ionospheric total electron content, reaching twice the normal values during the storm recovery phase, posing an unresolved question about its driving mechanism despite indications of disturbance electric fields. Xia et al. (2024) demonstrated that the ionospheric radial current exhibited an extreme response of approximately 15 nA/m^2 during the storm, with dawn-dusk asymmetry driven by the solar wind merging electric field. In this study, we performed a detailed analysis of the ionospheric zonal currents (including the EEJ) at low and middle latitudes during this storm, based on the magnetic measurements from ground-based magnetometers and ESA's Swarm satellite. With these observations, we would like to discuss the possible influences of PPEF and DDEF on the ionospheric zonal currents, especially their LT dependence.

2. Data and Approaches

2.1. Magnetic Measurements From Ground and Satellites

In this study, magnetometer data from a pair of ground-based stations, located at the American sector, have been analyzed, for representing the EEJ responses. Vector magnetic measurements from the equatorial station, Huancayo (HUA, −12.1° geographical latitude, −75.3°E geographic longitude, 1.2° MLat), and a low-latitude station, Piura (Y17, −5.2° geographical latitude, −80.6°E geographic longitude, 7.3° MLat) have been well calibrated and freely accessible on the website of SuperMAG (https://supermag.jhuapl.edu/mag/).

In addition, magnetic measurements from ESA's Swarm mission (Friis-Christensen et al., 2008) have also been used to calculate the ionospheric currents, especially to show the responses of zonal currents at low and middle latitudes. During this storm, the Swarm B satellite flew in the noon and midnight sectors, while the lower pair, Swarm A and C, flew in the dawn dusk sectors, which provides a good opportunity to check the zonal current responses at different LT sectors.

2.2. Ionospheric Zonal Currents Calculations

For calculating the EEJ from ground stations, we followed the approach introduced by Yamazaki et al. (2014) using the magnetic measurements from one pair of magnetometers. The daytime deviation of horizontal (H) components of the magnetic field, ΔH, with respect to the nightside (22:00–04:00 LT) mean level is defined as $\Delta H = B_H - B_{Hq}$, where the B_H is the H component of the magnetic field and the B_{Hq} is the nightside average value during the five mostly quiet days of this month. Therefore, the ΔH variations can be attributed to the magnetic effect of the dayside ionospheric current. The EEJ is then further calculated by EEJ $= \Delta H_e - \Delta H_l$, where ΔH_e and ΔH_l are the ΔH for the station near the dip equator and low latitude.

For the EEJ derived from the Swarm satellite, we used the Level-2 product. The detailed description of EEJ calculation from Swarm has been well documented by Alken et al. (2020). It is noted that the standard EEJ product is only provided during the 06:00–18:00 LT; therefore, no EEJ around 19:00 LT can be shown.

The along orbit magnetic measurements from Swarm satellites provide a possible way to derive the ionospheric zonal currents at middle and low latitudes. For that, we employ the approach introduced by Zhou and Lühr (2023). Considering the altitude of the E-region (110 km) and F2 peak (typically 300 km), the mean height of the zonal

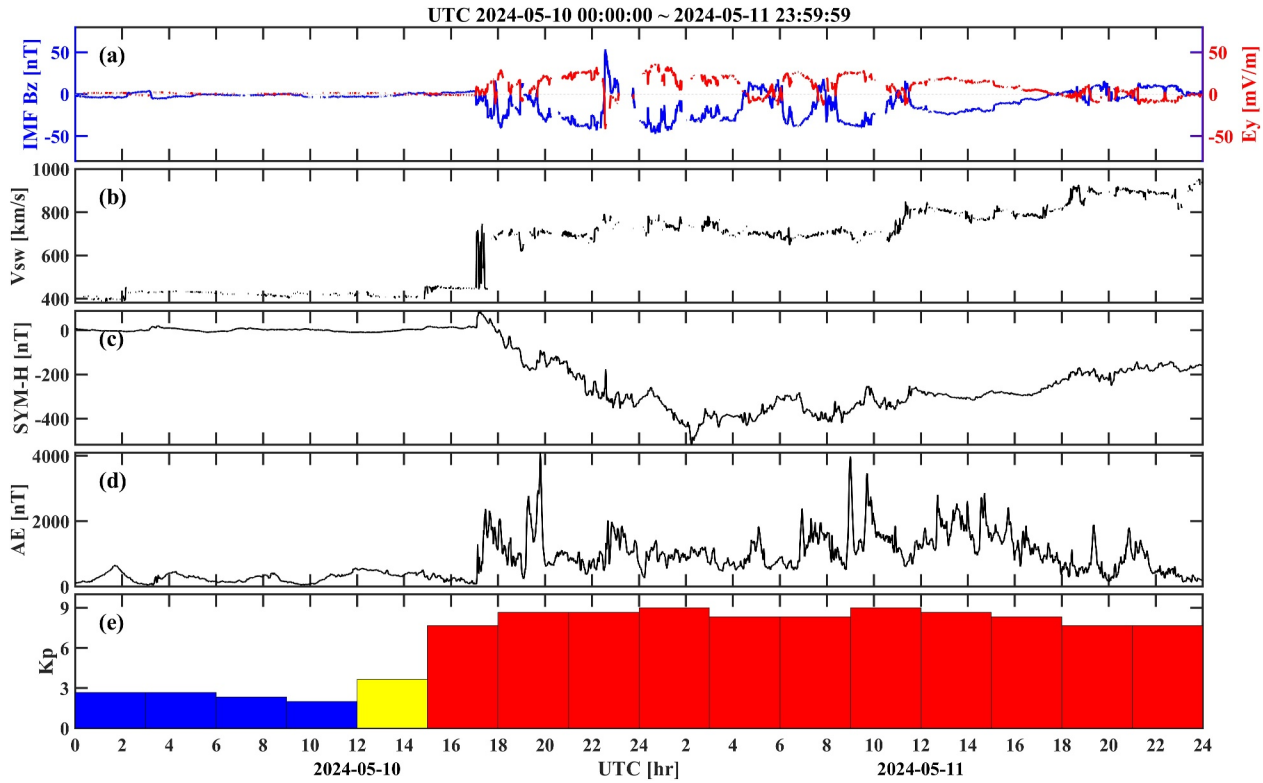

Figure 1. The variations of (a) IMF *Bz* and *Ey*, (b) solar wind velocity (*Vsw*), (c) *SYM-H*, (d) *AE*, and (e) 3-hour *Kp* indices during this storm.

current is assumed to flow at the middle height of 230 km. By assuming a series of east-west line currents separated by 2° in latitude within the ±50° Quasi-Dipole (QDlat, hereafter named as magnetic latitude, MLat) latitude range, the height-integrated current density can be derived from the vertical magnetic component. Basic equations and more details for the derivation of the current density can be found in Lühr et al. (2004) and Zhou and Lühr (2023).

We want to note that the EEJ has been normally assumed to flow at the E region ionospheric altitude, for example, around 110 km, while for the zonal current the mean height is assumed at a height of 230 km, by taking the middle altitude of the E-region (110 km) and F2 peak (typically 300 km). For calculating the zonal currents, both the northward (*Bx*) and vertical (*Bz*) components of *B* fields are needed. When there are zonal currents at both below and above the Swarm satellites, their contributions to the *Bx* component will be canceled, while adding on for the *Bz* components. Therefore, we followed the approach by Zhou et al. (2020) and used the vertical component *Bz* to calculate the zonal currents. It also means the zonal currents represent the height-integrated current density, including the contributions from both the E and F region currents.

3. Results

3.1. Overview of the Solar Wind and Magnetic Disturbance Indices During the Storm

Before showing the ionospheric zonal current responses, we first provided an overview of the solar wind and magnetic disturbance indices during the storm on 10–12 May 2024. From top to bottom, Figure 1 presents the variations of solar wind velocity (V_{sw}), IMF *Bz* and *Ey* in the geocentric solar-magnetospheric (GSM) coordinates, *SYM-H*, *AE* and 3-hr *Kp* indices during 10–12 May 2024. Enhanced magnetic activity started after the sudden increase of V_{sw} from 450 to 710 km/s at 17:00 coordinated universal time (UTC) on 10 May (see Figure 1b), which was accompanied by a sudden storm commencement (SSC) with *SYM-H* index increased from 10 to 78 nT (see Figure 1c). Afterward, the V_{sw} kept around 750 km/s, while the IMF was rather dynamic. Prominent southward *Bz* reached its first lowest value of −43 nT at 22:00 UTC, then suddenly turned northward and reached its largest value of 54 nT at 22:30 UTC, accompanied by an abrupt change in *Ey* from 31 to −40 mV/m (see Figure 1a). After

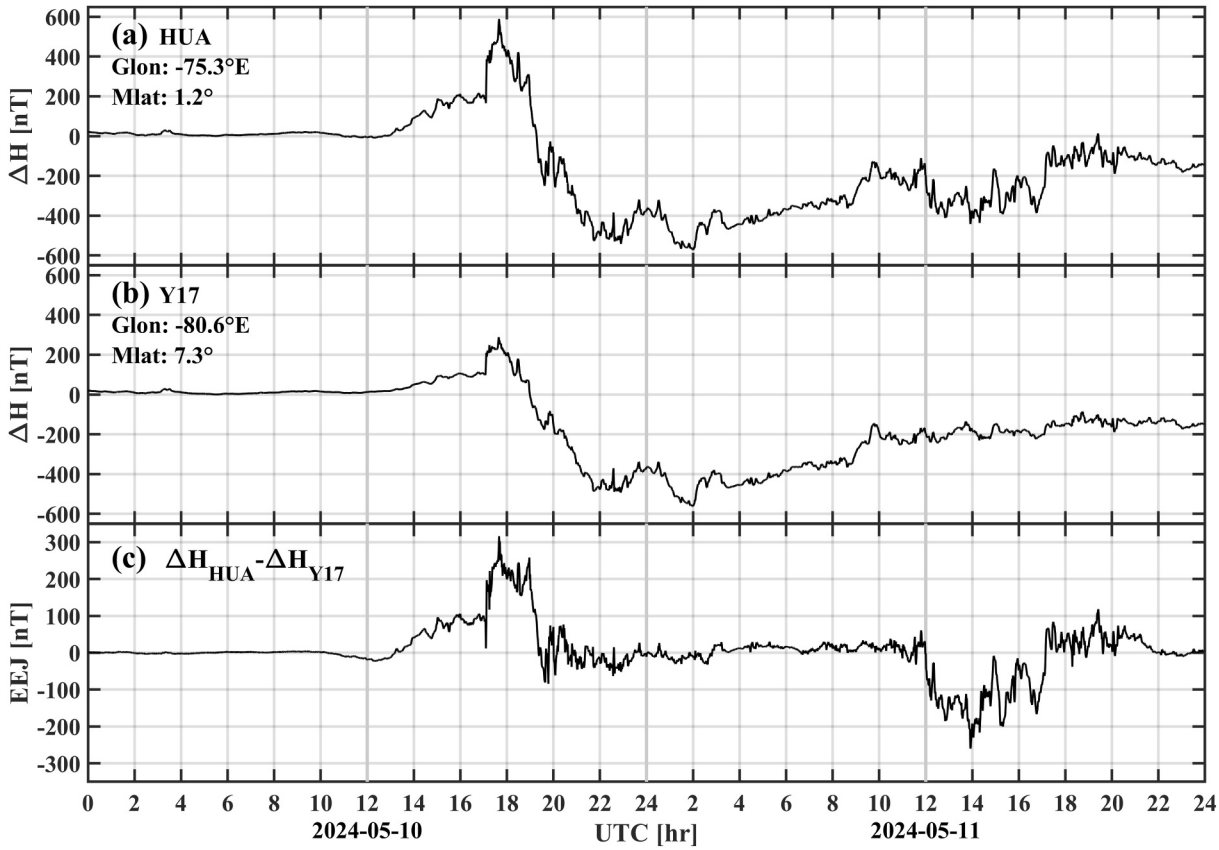

Figure 2. The variations of ΔH at ground stations (a) HUA and (b) Y17 in the American sector. The EEJ derived from the two stations is shown in the third panel.

the SSC, the *SYM-H* index continued to decrease and reached its minimum value of −518 nT around 02:00 UTC on 11 May, indicating the storm main phase. In the meanwhile, the *AE* index was also quite dynamic, reaching its highest value of 4,098 nT (see Figure 1d), and the *Kp* reached as high as 9 (see Figure 1e). Afterward, the *SYM-H* index slowly increased but with values below −150 nT, implying a long-lasting recovery phase of the storm. In the meanwhile, the V_{sw} kept at rather high values of 700–900 km/s, and the IMF three components also showed quite prominent disturbances, suggesting that energy input from the solar wind continues into the near-Earth space environment in the rest days.

3.2. EEJ Estimated From Ground Stations and Swarm Satellites

Figures 2a and 2b show the variations of ΔH at ground stations HUA and Y17 on 10–11 May 2024. Prior to 14:00 UTC on 10 May, ΔH values remained stable at low magnitudes. Subsequently, low-amplitude perturbations commenced from 13:00 UTC and persisted until 17:00 UTC. Following the SSC appeared at 17:00 UTC, ΔH from both stations exhibited a rapid increase, reaching peak values of 589 nT at HUA and 289 nT at Y17. This positive perturbation of ΔH persisted for about 4 hr, and then continued to decrease, reaching minima twice at about 22:00 UTC on 10 May and 02:00 UTC on 11 May, respectively. During the recovery phase, ΔH from HUA reached the third minimum of about −440 nT around 14:00 UTC on 11 May and persisted for about three hours, while Y17 didn't show conspicuous decrease and maintained magnitudes at about −200 nT. After 18:00 UTC on 11 May, ΔH of both stations steadily recovered to their quiet-period levels.

Figure 2c presents the EEJ derived from these pair stations. A pronounced enhancement occurred at about 17:00 UTC on 10 May and persisted for about 2 hr, synchronizing with the ΔH variation from the two stations. Considering the two stations were around noon local time at this period, the enhanced eastward EEJ after SSC is caused by the eastward PPEF, which agrees also well with the earlier statistic results that PPEF mainly directs eastward during daytime. Then, the EEJ started to decrease gradually and reached the first minimum of about −85 nT at 19:30 UTC. According to a previous study by Xiong et al. (2015), the westward disturbance winds need

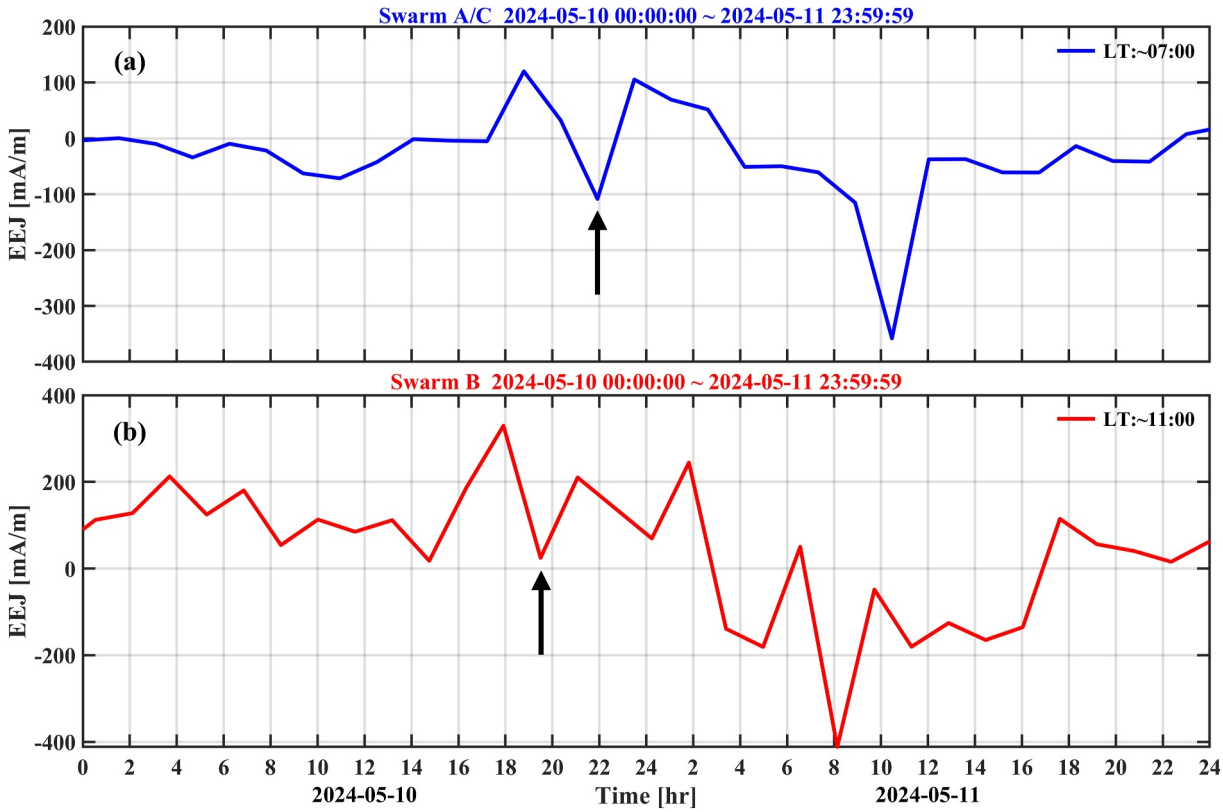

Figure 3. The variation of EEJ derived from the Swarm (a) A/C and (b) B.

about 3–4.5 hr to reach the equatorial latitude, further setting up the DDEF there. As the DDEF directs westward around noon, it is expected to see westward EEJ around 19:30 UTC (corresponding to 14:30 LT) when the DDEF is dominant at the equator. The above mentioned variations of EEJ agree well with the polarities of PPEF and DDEF during daytime hours. After 19:30 UTC, EEJ started to recover to its quiet-time level, and stayed around zero until 12:00 UTC on the next day. From then we see the EEJ directed mainly westward, reaching its minimum value of about −260 nT at 14:00 UTC on 11 May. The westward EEJ corresponds well to the negative ΔH values observed by HUA but not by Y17, even if they are separated by on 6° MLat. The difference between the two stations suggested that the westward EEJ was quite narrow in latitude, and was confined above the magnetic equator. This westward EEJ started to appear at 12:00 UTC (corresponding to about 07:00 LT) and persisted for about 5 hr. The IMF *Bz* was mainly southward and solar wind *Ey* was positive during this period, which should cause an eastward PPEF on the dayside in the equatorial region. Therefore, the prominent westward EEJ during the 5 hr can not be attributed to PPEF.

Figures 3a and 3b show the EEJ estimates from the Swarm A/C and Swarm B, respectively. It is noted that for the lower pair of Swarms, we used the average EEJ values of Swarms A and C. When examining the EEJ variations with the storm development, a prominent feature is that mainly the enhanced eastward EEJs were observed from 16:00 UTC on 10 May to 02:00 UTC on the next day (except the EEJ from Swarm A/C around 22:00 UTC on 10 May), and afterward the westward EEJs were dominated until 16:00 UTC on 11 May. This feature of EEJ is quite consistent between Swarm A/C and Swarm B, though slight time lags were seen between their peaks of eastward/westward currents. For example, the eastward peaks first appeared at about 19:00 and 18:00 UTC on 10 May for the dawn and noon sectors, while the westward peaks appeared at 08:00 UTC and 10:30 UTC on 11 May for the two local time sectors.

Quite impressively, the most intense eastward and westward EEJ reached over 300 mA/m and −400 mA/m from Swarm observations. As shown in Figure 4, such intense EEJ values have never been observed by Swarm satellites during their past 11-year flying period for the corresponding LT sectors. Even during the very intense disturbance caused by the Tonga eruption event, the westward EEJ only reached about the −180 nT (see Figure 1f

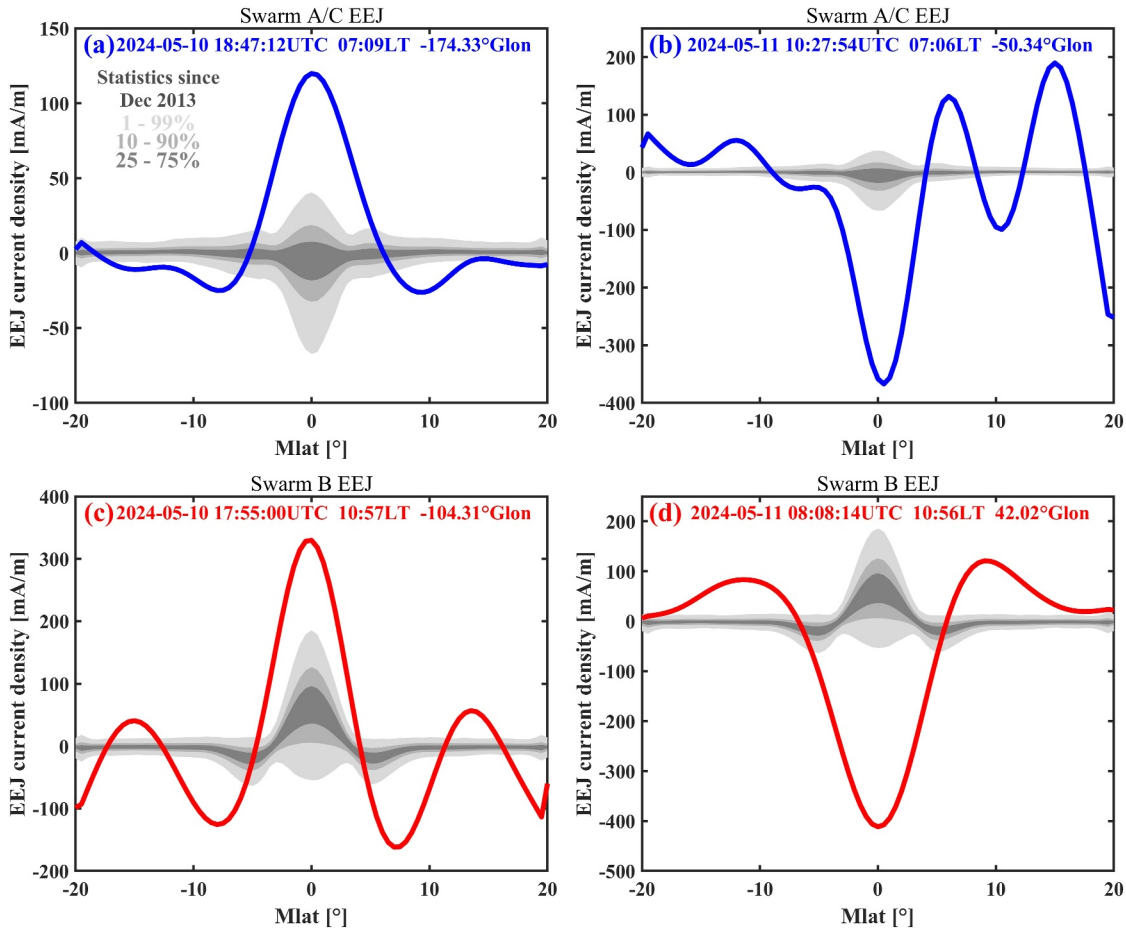

Figure 4. Latitudinal profiles of the most intense (left) eastward and (right) westward EEJs from the (top) Swarm A/C and (bottom) Swarm B satellites.

of Harding et al., 2022). As shown from the percentage distributions in Figure 4, the EEJ around 07:00 LT are mostly rather weak, and sometimes event westward. Shortly after the SSC (left columns), the EEJ from Swarms A and C, with a value of 135 mA/m, is in fact 4–5 times larger than the largest values in this LT sector; while for Swarm B, around 11:00 LT, it reached a value of 300 mA/m, which is also as twice as the largest quiet-time value. During the storm main phase (right columns), both satellites observed westward EEJ reaching about −400 mA/m, that is by a factor larger than the quiet-time values.

Another feature of EEJ is that not only the intensity has been largely enhanced but also the latitudinal width of EEJ has been largely enhanced. As seen from Figures 4a and 4c, the quiet-time return current (or side-band) of EEJ is located at about ±5° MLat, while the side-band for the two considered orbits after SSC has expanded to ±8° MLat. As a result, the intensity of the side-band currents has also been largely enhanced. A similar situation applies for the storm main phase, where both the intensity and width of EEJ have been largely enhanced. In addition, for some orbits the EEJ profile has been disturbed, for example, Figure 4b, which suggests that additional currents should exist in the magnetosphere/ionosphere during this intense storm. In this way, additional modification might be needed during magnetic disturbed periods for the widely used EEJ calculating approaches from low Earth orbit (LEO) satellites (e.g., Alken et al., 2020; Lühr et al., 2004).

3.3. Zonal Currents at Low and Middle Latitudes Estimated From Swarm

Next, we show the zonal current estimates from the Swarm satellites at low and middle latitudes. To reduce possible influences from the high latitude currents, we focused only on zonal currents within ±45° MLat, and the results are shown in Figure 5. As there is almost no zonal current around midnight (e.g., Zhou et al., 2020), for Swarm B only the current around noon has been shown (Figure 5a). One prominent feature at this LT sector is that

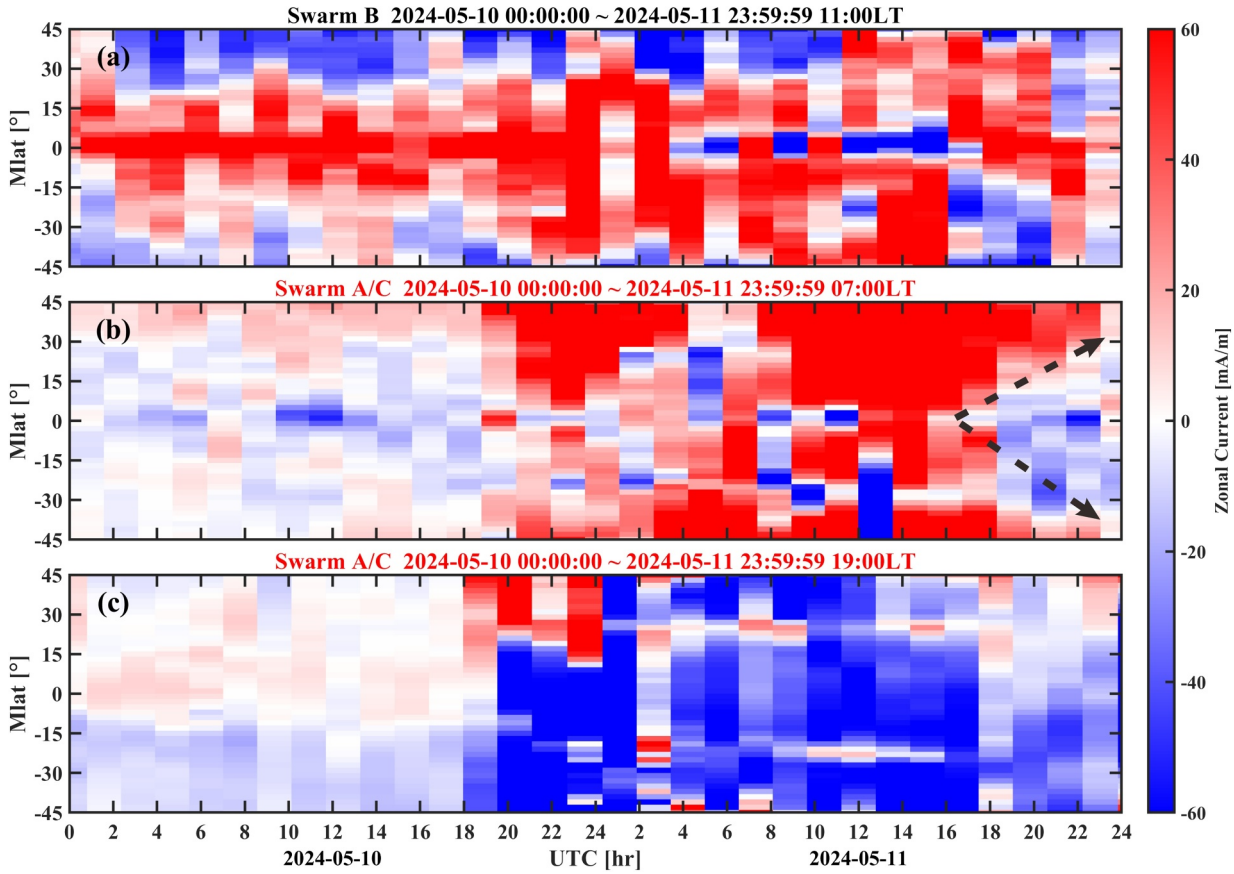

Figure 5. The zonal current estimates from the Swarm satellites at low and middle latitudes.

within ±30° MLat the zonal current directed mainly eastward, while beyond 30° MLat it directed westward. In addition, the eastward zonal current seems to slightly extend to higher MLat during the storm main phase. One exception is that from 04:00–18:00 UTC on 11 May, a clear westward zonal current jet appeared above the equator, corresponding to the westward EEJ during this period, as shown in Figure 3.

Similar to EEJ, for the lower pair, Swarms A and C, flying side-by-side, we used the average value of zonal currents of the two satellites. As seen, the zonal currents at dawn and dusk sides showed quite different storm responses. Before the storm, the currents within ±30° MLat directed mainly westward and eastward at dawn and dusk sides, respectively. However, right after the SSC (since 18:00 UTC on 10 May) enhanced eastward currents were dominated in the dawn sector, covering the low and middle latitudes; conversely, enhanced westward currents were observed in the dusk sector, extending also to middle latitudes. Compared to the geomagnetically quiet values, the eastward/westward currents for the two LT sectors were enhanced by a factor during the storm. In addition to this main feature, the zonal currents during storm showed also latitudinal and shorter period variations. For example, for the dawn sector, transient westward currents were also observed at some latitudes during the storm main phase (00:00–12:00 UTC on 11 May). For the dusk sector, eastward zonal currents were observed in the northern middle latitudes shortly after SCC (between 18:00–23:00 UTC on 10 May), and two eastward current jets around ±25° MLat were observed to be immersed in the westward currents during the main and recovery phases (between 02:00–14:00 UTC on 11 May).

4. Discussions

4.1. Responses of EEJ to the Solar Wind Energy Input

One interesting question we want to address is that after SSC the solar wind velocity has been enhanced and kept at the level of 700–800 km/s, and the meanwhile IMF Bz component was also quite dynamic for the rest one and a

half days; however, there were mainly two active periods caused prominent perturbations of EEJ, as seen from the magnetic measurements from both the ground and Swarm satellites. During the first period, enhanced eastward EEJs were first observed around 18:00–19:00 UTC shortly after the SSC, which agree well with the eastward PPEF on the dayside. The follow-up DDEF caused westward EEJs have been well captured by the ground stations, which were also seen around 19:30 and 22:00 UTC for Swarm B and Swarm A/C, respectively. During the second active period, mainly westward EEJs were observed by the ground stations from 12:00 to 18:00 UTC on 11 May. When looking at the westward peaks from the satellite, they appeared at about 08:00 and 10:30 UTC from Swarm B and Swarm A/C. We speculate that the reason for the 4 and 1.5 hr advance of westward EEJs observed by Swarm satellites should be the differences in local time and longitudes between these observations. Nevertheless, the mainly westward EEJ direction remained the same during this second active period between Swarm satellites and ground measurements.

In previous studies (e.g., Kelley et al., 2003; Kikuchi et al., 1996; Yu & Ridley, 2009), the southward IMF Bz turning has often been used as an indicator for representing the magnetic reconnection during which enhanced solar wind energy is expected to enter the magnetosphere and ionosphere. Therefore, the PPEF from the high latitude to middle and low latitudes is expected to occur under southward Bz conditions. During this intense storm, prominent southward turning of IMF Bz (or negative Ey) has been observed several times. However, when the mostly intense southward Bz appeared around 00:00 UTC on 11 May, no prominent EEJ responses were observed at low and equatorial latitudes. For the second active period of EEJ, for example from 12:00 to 18:00 UTC on 11 May for the ground stations, the southward turning of Bz during this period is expected to cause eastward PPEF on the dayside equatorial region, which further drives the eastward EEJ. Usually, the PPEF is a short-term phenomenon, lasting typically less than 1 hr. If the EEJ is mainly driven by PPEF, it is expected that the EEJ changes its polarity accordingly with IMF Ey variations. However, only intense westward EEJs were observed. From this point of view, it seems that the IMF Bz itself alone might not be the best indicator for representing the equatorial ionospheric responses to the enhanced solar wind input during geomagnetic storms. One might suggest that the DDEF during this period should be the reason for the intense westward EEJ on the dayside. When looking at the indices shown in Figure 1, enhanced AE index was observed from 07:00 to 18:00 UTC, suggesting enhanced auroral electrojet caused by the substorm. Usually enhanced Joule heating is expected during enhanced auroral electrojet, which causes the expansion of neutral atmosphere. As a consequence, the equatorial neutral winds are formed and propagate to the equatorial wind, further causing westward DDEF on the dayside equatorial region.

4.2. Responses of Ionospheric Zonal Currents at Low and Middle Latitudes: LT Dependences

As pointed out, the EEJ responses to geomagnetic storms have been widely investigated by previous studies, but the zonal currents at low and middle latitudes during storms have not been reported before. During this storm event, the three Swarm satellites provide a very good opportunity to check the LT responses of zonal currents at low and middle latitudes.

As shown in Figure 5, the intensified eastward zonal currents at noon and dawn sectors, shortly after the SSC of the storm, should be mainly caused by PPEF. Similarly, general enhanced eastward EEJ have been observed by both Swarm satellites for the two LT sectors, except the orbit from Swarm A and C around 22:00 UTC on 10 May showing westward EEJ (Figure 3). In addition, the zonal current responses show prominent dependence on LT. For example, at the dusk sector (around 19:00 LT as shown in Figure 5c), mainly westward zonal currents have been observed shortly after the SSC, which should also be related to the PPEF. This is somehow different from the previously reported LT dependence of PPEF by Fejer et al. (2008), who suggested that the PPEF changes from eastward to westward around 21:00 LT. One possible reason could be that their results are derived based on a statistical survey on several-year vertical plasma drift data from the ROCSAT-1 satellite, representing the average character of the PPEF during storms, while our result applies to the most intense storm happened in the past 20 years.

At the storm recovery phase when the DDEF dominated (after 02:00 UTC on 11 May), the CEJ with unprecedented values (reaching −400 mA/m) at both the noon and dusk sectors were observed. The westward CEJ agrees well with the theorem that the DDEF directs mainly westward during daytime. Such enhanced CEJ around the noon sector during storm times has been reported by earlier studies (e.g., Zhou et al., 2018), and has been attributed to enhanced westward disturbance winds. For the zonal currents, a similar westward current jet above the equator was observed during 04:00–18:00 UTC on 11 May by Swarm B around the noon sector, suggesting that the westward disturbance wind dominated the equator during this time period. For the dawn sector, westward

zonal currents above the equator were only observed occasionally for several orbits (Figure 5b), which was not as prominent as that of CEJ (Figure 3b) at the same LT sector. Considering the approaches for estimating the EEJ and zonal currents, these observations imply that the DDEF or disturbance winds might change direction between the E and F region altitudes at the dawn sector. It is a pity that we don't have neutral wind measurements at different altitudes during this event. But based on the horizontal winds from the Ionospheric Connection Explorer (ICON) satellite during another storm on 25–26 August 2021, Wu et al. (2024) reported that both the meridional and zonal winds showed distinguishable vertical shear structures at different stages of the storm. During the storm main phase, on the dayside, the peak velocities of westward winds extended from a higher altitude to a lower altitude, whereas during the recovery phase, the peak velocities of westward winds extended from lower altitudes to higher altitudes. Statistical analysis of the wind measurements from ICON also reveals that vertical shears of both zonal and meridional winds have been often observed from ionospheric E and F regions (e.g., England et al., 2022; Huang et al., 2023).

Another indication of the DDEF effect on the zonal currents is that during the storm recovery phase, the decrease of eastward current first appeared at the equator and then gradually extended to low and middle latitudes (indicated by the dashed-black arrows during 16:00–24:00 UTC on 11 May). It can be reasonably explained that during the storm recovery phase, the decrease of disturbance westward winds first appears at the equatorial region, and then the reduction of disturbance winds gradually extends to low and middle latitudes when there is no further solar wind energy input into the auroral region.

4.3. Enhanced Eastward Current Jets at Middle Latitudes

As shown in Figure 5, two narrow eastward current jets at about ±25° MLat were observed in the 19:00 LT sector during storm main and recovery phases, which were immerged in the westward currents at the other latitudes for this LT sector. To our knowledge, this is the first report of such narrow current jets at middle latitudes. The eastward current jet started to appear around 02:00 UTC on 11 May, which is almost the same time as the westward current jets above the equator appeared at the 11:00 LT (Figure 5a). In addition, both current jets disappear in 16:00 UTC on 11 May. Following the generation mechanism for the CEJ, which involves the westward neutral winds (Raghavarao & Anandarao, 1980; Somayajulu et al., 1993), we suggest that the disturbance winds could be the driver to cause the eastward jets at middle latitudes. Though we could not provide direct evidence, we speculate that eastward wind jets might exist at about ±25° MLat around dusk sector.

Even more interestingly, we found corresponding plasma density (*Ni*) bumps near ±25° MLat associated with the eastward current jets when they first appeared (Figure 6). However, these *Ni* bumps disappeared and only an *Ni* peak near the equator showed up. We want to note that the narrow eastward electrojets around ±25° MLat observed by the Swarm persisted for about 12 hours, during 02:00–14:00 UTC on 11 May. During this period, the Swarm orbits shifted from the American sector to the Asian sector. As already reported in a previous study, during this storm, the ionospheric plasma density showed prominent longitudinal asymmetry (e.g., Li et al., 2024; Zhang et al., 2024), which might also contribute to the longitudinal difference of Swarm observed eastward zonal current jets around ±25° MLat. The changing relation between ionospheric zonal currents and plasma density, maybe also the zonal winds, suggests that the coupling between neutrals and plasma is quite complicated, especially during magnetic disturbed periods. Further simulation studies are encouraged to reveal the involved processes.

5. Summary

In this study, we investigate the ionospheric zonal currents from equatorial to middle latitudes during a very intense geomagnetic storm on 10–12 May 2024, by combining the magnetic measurements from ground stations and Swarm satellites. The main findings are summarized below.

1. Ground and Swarm satellite observations recorded unprecedented intense EEJ during this storm; extreme eastward and westward EEJ values reached 300 and −400 mA/m during the storm main and recovery phases, respectively. The eastward enhancement of EEJ appeared shortly after the SSC, mainly caused by the PPEF. The extreme westward EEJ during the storm recovery phase should be related to the DDEF, and we suggest that the disturbance winds were caused by the enhanced substorm activities.
2. The zonal currents at low and middle latitudes exhibited distinct LT dependence. In the noon sector, eastward currents were dominated under both quiet and storm conditions, with slight intensification during the storm. Conversely, the zonal currents in the dawn and dusk sectors displayed abrupt current reversals within 30 min

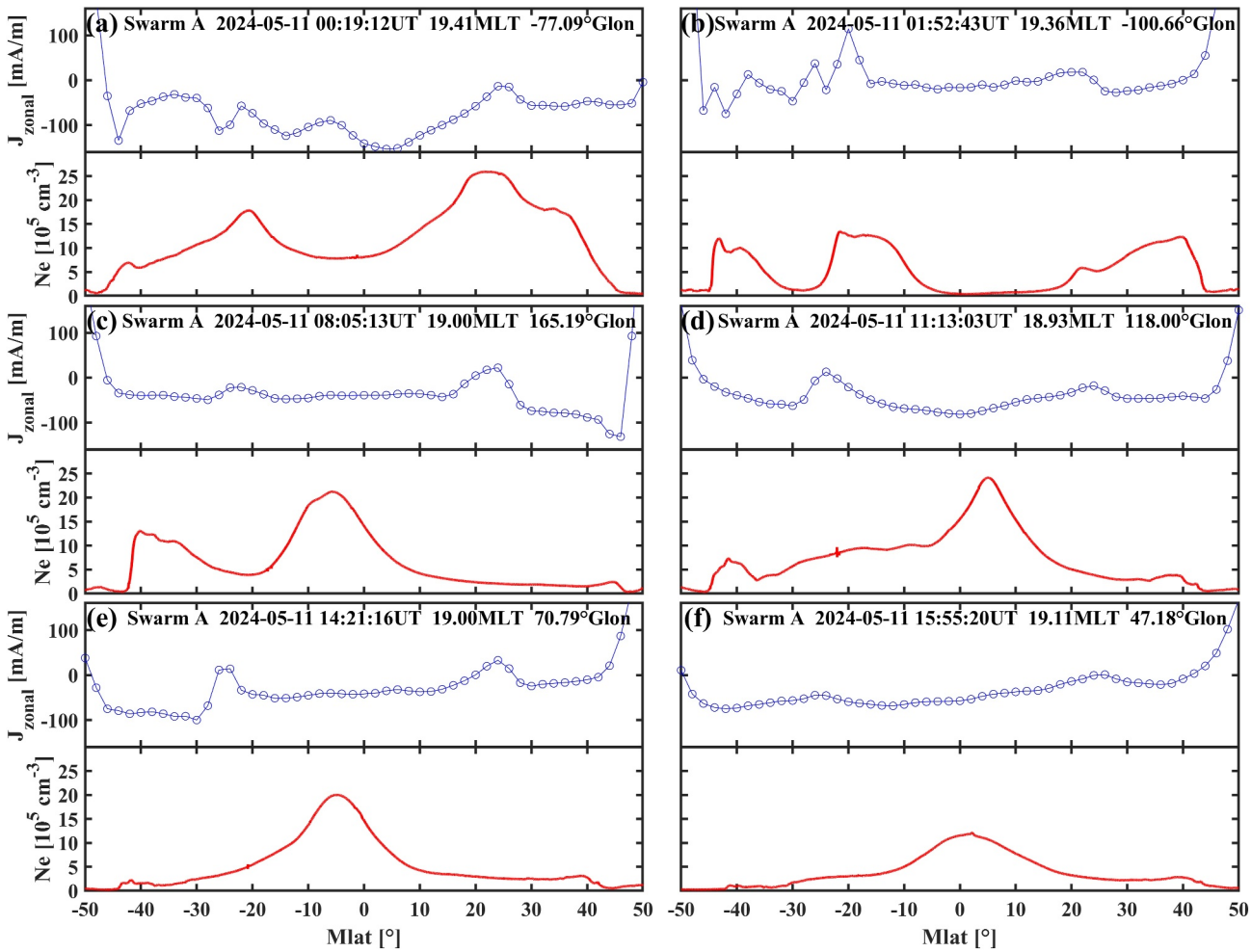

Figure 6. The latitude profile of (blue) zonal currents as well as (red) the corresponding plasma density measured by the Langmuir probe onboard Swarm A, at different storm phases on 11 May 2024. The time for Swarm A crossing equator is (a) 00:19:12 UT, (b) 01:52:43 UT, (c) 08:05:13 UT, (d) 11:13:03 UT, (e) 14:21:16 UT, (f) 15:55:20 UT.

after the SSC, characterized by sustained eastward (dawn) and westward (dusk) perturbations persisting for the rest of one and a half days. In addition to LT, the zonal currents showed dependence on latitude.

3. During the storm main and recovery phases, two eastward zonal current jets were found located at ±25° magnetic latitudes at the dusk sector emerged with westward zonal currents at other low and middle latitudes. To our knowledge, this is the first report of such narrow current jets at middle latitudes during storms.

Data Availability Statement

We want to thank SuperMAG and ESA for providing the ground-based and satellite magnetic measurements. The ground-based magnetometer data can be downloaded from https://supermag.jhuapl.edu/mag/. The Swarm data can be downloaded at the ESA website (https://earth.esa.int/web/guest/swarm/data-access). IMF Bz, Ey, solar wind velocity, SYM-H and AE data are accessed via OMNIWeb (https://omniweb.gsfc.nasa. gov/form/omni_-min.html). The Kp index is provided by the World Data Center for Geomagnetism, Kyoto (https://wdc.kugi.kyoto-u.ac.jp).

Acknowledgments
This work is supported by the National Natural Science Foundation of China (42474200 and 42174186) and the National Key R&D Program of China (Grant 2022YFF0503700). Chao Xiong is supported by the Dragon 6 cooperation 2024–2028 (project no. 95437). This study is supported by "the Fundamental Research Funds for the Central Universities (2042025kf0026)."

References

Alken, P. (2020). Estimating currents and electric fields at low latitudes from satellite magnetic measurements. In M. Dunlop & H. Lühr (Eds.), *Ionospheric multi-spacecraft analysis tools: Approaches for deriving ionospheric parameters* (pp. 233–254). Springer International Publishing. https://doi.org/10.1007/978-3-030-26732-2_11

Blanc, M., & Caudal, G. (1985). The spatial distribution of magnetospheric convection electric fieldsat ionospheric altitudes: A review. II. Theories. *Annales Geophysicae*, *3*, 27–42.

Blanc, M., & Richmond, A. d. (1980). The ionospheric disturbance dynamo. *Journal of Geophysical Research*, *85*(A4), 1669–1686. https://doi.org/10.1029/JA085iA04p01669

Carmo, C. S., Dai, L., Wrasse, C. M., Barros, D., Takahashi, H., Figueiredo, C. A. O. B., et al. (2024). Ionospheric response to the extreme 2024 Mother's Day geomagnetic storm over the Latin American sector. *Space Weather*, *22*(12), e2024SW004054. https://doi.org/10.1029/2024SW004054

England, S. L., Englert, C. R., Harding, B. J., Triplett, C. C., Marr, K., Harlander, J. M., et al. (2022). Vertical shears of horizontal winds in the lower thermosphere observed by ICON. *Geophysical Research Letters*, *49*(11), e2022GL098337. https://doi.org/10.1029/2022GL098337

Fejer, B. G., Jensen, J. W., & Su, S.-Y. (2008). Seasonal and longitudinal dependence of equatorial disturbance vertical plasma drifts. *Geophysical Research Letters*, *35*(20). https://doi.org/10.1029/2008GL035584

Friis-Christensen, E., Lühr, H., Knudsen, D., & Haagmans, R. (2008). Swarm—An Earth observation mission investigating geospace. *Advances in Space Research*, *41*(1), 210–216. https://doi.org/10.1016/j.asr.2006.10.008

Harding, B. J., Wu, Y.-J. J., Alken, P., Yamazaki, Y., Triplett, C. C., Immel, T. J., et al. (2022). Impacts of the January 2022 Tonga volcanic eruption on the ionospheric dynamo: ICON-MIGHTI and Swarm observations of extreme neutral winds and currents. *Geophysical Research Letters*, *49*(9), e2022GL098577. https://doi.org/10.1029/2022GL098577

Heppner, J. P. (1972). Polar-cap electric field distributions related to the interplanetary magnetic field direction. *Journal of Geophysical Research (1896–1977)*, *77*(25), 4877–4887. https://doi.org/10.1029/JA077i025p04877

Huang, F., Lei, J., Zhang, S.-R., Wang, Y., Li, Z., Zhong, J., et al. (2024). Peculiar nighttime ionospheric enhancements over the Asian sector during the May 2024 superstorm. *Journal of Geophysical Research: Space Physics*, *129*(11), e2024JA033350. https://doi.org/10.1029/2024JA033350

Huang, Y., Xiong, C., Wu, J., Stolle, C., Wang, F., Zheng, Y., et al. (2023). Dayside vertical wind reversal at transition altitude from E to F regions observed by the ICON satellite. *Earth and Space Science*, *10*(5), e2023EA002836. https://doi.org/10.1029/2023EA002836

Kelley, M. C., Makela, J. J., Chau, J. L., & Nicolls, M. J. (2003). Penetration of the solar wind electric field into the magnetosphere/ionosphere system. *Geophysical Research Letters*, *30*(4). https://doi.org/10.1029/2002GL016321

Kikuchi, T., Lühr, H., Kitamura, T., Saka, O., & Schlegel, K. (1996). Direct penetration of the polar electric field to the equator during a DP 2 event as detected by the auroral and equatorial magnetometer chains and the EISCAT radar. *Journal of Geophysical Research*, *101*(A8), 17161–17173. https://doi.org/10.1029/96JA01299

Le Huy, M., & Amory-Mazaudier, C. (2005). Magnetic signature of the ionospheric disturbance dynamo at equatorial latitudes: "Ddyn.". *Journal of Geophysical Research*, *110*(A10). https://doi.org/10.1029/2004JA010578

Li, W., Liu, L., Yang, Y., Han, T., Du, R., Zhang, R., et al. (2024). Interhemispheric and longitudinal differences in the ionosphere–thermosphere coupling process during the May 2024 superstorm. *Earth and Planetary Physics*, *8*(6), 910–919. https://doi.org/10.26464/epp2024073

Lühr, H., Maus, S., & Rother, M. (2004). Noon-time equatorial electrojet: Its spatial features as determined by the CHAMP satellite. *Journal of Geophysical Research*, *109*(A1). https://doi.org/10.1029/2002JA009656

Manoj, C., & Maus, S. (2012). A real-time forecast service for the ionospheric equatorial zonal electric field. *Space Weather*, *10*(9). https://doi.org/10.1029/2012SW000825

Nishida, A. (1968). Coherence of geomagnetic DP 2 fluctuations with interplanetary magnetic variations. *Journal of Geophysical Research (1896–1977)*, *73*(17), 5549–5559. https://doi.org/10.1029/JA073i017p05549

Raghavarao, R., & Anandarao, B. G. (1980). Vertical winds as a plausible cause for equatorial counter electrojet. *Geophysical Research Letters*, *7*(5), 357–360. https://doi.org/10.1029/GL007i005p00357

Scherliess, L., & Fejer, B. G. (1997). Storm time dependence of equatorial disturbance dynamo zonal electric fields. *Journal of Geophysical Research*, *102*(A11), 24037–24046. https://doi.org/10.1029/97JA02165

Somayajulu, V. V., Cherian, L., Rajeev, K., Ramkumar, G., & Reddi, C. R. (1993). Mean wind and tidal components during counter electrojet events. *Geophysical Research Letters*, *20*(14), 1443–1446. https://doi.org/10.1029/93GL00088

Wu, J., Xiong, C., Huang, Y., & Zhou, Y. (2024). Vertical gradients of neutral winds observed by ICON and estimated by the Horizontal Wind Model during the geomagnetic storm on August 26–28, 2021. *Earth and Planetary Physics*, *9*(1), 69–80. https://doi.org/10.26464/epp2024033

Xia, H., Wang, H., & Zhang, K. (2024). Extreme responses of the ionospheric radial currents to the main phase of the super geomagnetic storm on 10 May 2024. *Journal of Geophysical Research: Space Physics*, *129*(12), e2024JA033126. https://doi.org/10.1029/2024JA033126

Xiong, C., Lühr, H., & Fejer, B. G. (2015). Global features of the disturbance winds during storm time deduced from CHAMP observations. *Journal of Geophysical Research: Space Physics*, *120*(6), 5137–5150. https://doi.org/10.1002/2015JA021302

Xiong, C., Lühr, H., & Fejer, B. G. (2016). The response of equatorial electrojet, vertical plasma drift, and thermospheric zonal wind to enhanced solar wind input. *Journal of Geophysical Research: Space Physics*, *121*(6), 5653–5663. https://doi.org/10.1002/2015JA022133

Yamazaki, Y., & Kosch, M. J. (2015). The equatorial electrojet during geomagnetic storms and substorms. *Journal of Geophysical Research: Space Physics*, *120*(3), 2276–2287. https://doi.org/10.1002/2014JA020773

Yamazaki, Y., Richmond, A. D., Maute, A., Wu, Q., Ortland, D. A., Yoshikawa, A., et al. (2014). Ground magnetic effects of the equatorial electrojet simulated by the TIE-GCM driven by TIMED satellite data. *Journal of Geophysical Research: Space Physics*, *119*(4), 3150–3161. https://doi.org/10.1002/2013JA019487

Yu, Y., & Ridley, A. J. (2009). Response of the magnetosphere-ionosphere system to a sudden southward turning of interplanetary magnetic field. *Journal of Geophysical Research*, *114*(A3). https://doi.org/10.1029/2008JA013292

Zhang, R., Liu, L., Yang, Y., Li, W., Zhao, X., Yoshikawa, A., et al. (2024). Ionosphere responses over Asian-Australian and American sectors to the 10–12 May 2024 superstorm. *Journal of Geophysical Research: Space Physics*, *129*(12), e2024JA033071. https://doi.org/10.1029/2024JA033071

Zhou, Y., & Lühr, H. (2023). Average ionospheric Mid- and low-latitude currents from E- and F-region altitudes, derived by the Swarm constellation. *Journal of Geophysical Research: Space Physics*, *128*(6), e2022JA031234. https://doi.org/10.1029/2022JA031234

Zhou, Y., Lühr, H., & Alken, P. (2020). Average ionospheric middle and low latitudes nighttime zonal currents deduced from CHAMP. *Journal of Geophysical Research: Space Physics*, *125*(8), e2019JA027702. https://doi.org/10.1029/2019JA027702

Zhou, Y., Lühr, H., Xu, H., & Alken, P. (2018). Comprehensive analysis of the counter equatorial electrojet: Average properties as deduced from CHAMP observations. *Journal of Geophysical Research: Space Physics*, *123*(6), 5159–5181. https://doi.org/10.1029/2018JA025526